Isothermal Martensitic Transformation in a 12Cr-9Ni-4Mo-2Cu Stainless Steel in applied Magnetic Fields

D. San Martín[1], K. W. P. Aarts[1], P. E. J. Rivera-Díaz-del-Castillo[1], N. H. van Dijk[2], E. Brück[3] and S. van der Zwaag[1]

[1]Fundamentals of Advanced Materials Group, Faculty of Aerospace Engineering, Delft University of Technology, Kluyverweg 1, 2629 HS Delft, The Netherlands.

[2]Fundamental Aspects of Materials and Energy group, Faculty of Applied Sciences, TU Delft, Mekelweg 15, 2629 JB Delft, The Netherlands.

[3]Van der Waals-Zeeman Institute, University of Amsterdam, Valcknierstraat 65, 1018 XE Amsterdam, The Netherlands.

(NOTE: Since 2008, David San Martín works in the National Centre for Metallurgical Research, CENIM-CSIC, Madrid, Spain, dsm@cenim.csic.es)

Corresponding author:

Name: David San Martin

Postal Address: Faculty of Aerospace Engineering, Delft University of Technology, Kluyverweg 1, 2629 HS Delft, The Netherlands.

E-mail: d.sanmartin@tudelft.nl, dsm@cenim.csic.es

Telephone: 0031 15 27 84559

Fax: 0031 15 27 84472 (Netherlands)

Abstract:

This work concerns an in-situ study of the isothermal formation of martensite in a stainless steel under the influence of magnetic fields up to 9 T at three different temperatures (213, 233 and 253 K). It is shown that the presence of a constant applied magnetic field promotes the formation of martensite significantly. The activation energy for the nucleation of martensite has been derived using a semi-empirical kinetic model. The experimental results have been analyzed using the Ghosh and Olson model. While this model describes the time and field dependences of the experimental data well, the thermal frictional energy and the defect size values are much lower than those expected from earlier work.

PACS codes: 75.50.Bb, 64.70.Kb, 64.60.My.

Keywords: Stainless Steel, Magnetic field, Martensite, Austenite, Phase Transformations.

1. Introduction

Martensitic transformations (MTs) were first observed in iron based alloys. The main features of the martensitic transformation are its diffusionless nature (absence of concentration changes) and the cooperative mechanism of transformation (ordered collective movement of atoms over distances smaller than interatomic distances between iron atoms). From a kinetic point of view, martensitic transformations can be defined as athermal or isothermal. Athermal martensitic transformations (AMT) are time independent and controlled by the actual transformation temperature M_S [1-2]. Isothermal martensitic transformations (IMT) also occur below a critical temperature M_S but the nucleation process develops gradually with time at a constant temperature [3-7]. The growth of the martensitic crystal units is considered to be as fast as for the AMT. The overall IMT kinetics of the transformation can be described by a C curve similar to those used for describing diffusional transformations in steels. The isothermal martensite formation occurs in a wide range of highly alloyed steels, but is of particular interest for a range of precipitation hardening carbon poor CrNiMo stainless steels where the transformation is used to create a large microstructural refinement. This fine microstructure promotes the formation of nanoprecipitates with a resulting combination of a high strength and good toughness [8, 9].

According to previous investigations, in the present steel (Fe-12Cr-9Ni-4Mo) the isothermal martensite formation can take place by setting a constant temperature below M_S at sub-zero (below 0 ºC) temperatures [10, 11]. The isothermal martensite has been observed to form over a wide range of temperatures, with the nose of the C curve located

at 233 K [12]. The maximum volume fraction of martensite that forms during the isothermal transformation is around 0.7 [10, 11].

Several authors have observed that the MTs can also be stimulated by combining cooling treatments with additional external stimuli such as hydrostatic pressure, plastic deformation or magnetic fields [10, 13-20]. Earlier work on the stainless steel also studied here has shown that magnetic fields do indeed accelerate the transformation [17]. Work on other stainless steels has shown that the nose of the curve can be shifted to lower temperatures and shorter times by applying strong magnetic fields [15, 20]. However, in all studies, the starting microstructure was kept constant and its effect on the kinetics of the martensite was not studied. In the present steel two different initial microstructures, three different isothermal transformation temperatures and 5 different magnetic field intensities have been combined to study the influence of magnetic fields on the IMT. Such a wide range of conditions has not yet been applied in earlier studies on field stimulated martensitic transformations in stainless steels. The experimental results have been quantitatively analyzed using a semi empirical model as well as a modified version of the Ghosh and Olson model for martensitic transformations [3, 4].

2. Materials and Experiments

The composition of the steel studied in this work is given in Table 1. The as-received material was produced in plates of 310 mm width × 0.5 mm thickness. The main phases present in the starting as-received microstructure are austenite, the chi-phase ($Fe_{32}Cr_{12}Mo_{10}$) [21] and a small amount of martensite [22]. The chi-phase has a complex cubic structure (CBCC-A12, α-Mn type of BCC) [23] and is often found in stainless

steels alloyed with high concentrations of molybdenum. Two different kinds of samples were used during this investigation; a) non heat treated as-received samples (NHT) and b) heat treated samples (HT). For the heat treatment, a vacuum furnace (Cambridge Vacuum Engineering type HLFC 1218) with a horizontal loading chamber was used. The HT samples were slowly heated at 15 K/min to 1223 K, kept for 10 s, and quenched at 900 K/min to room temperature. Aim of the heat treatment was to retransform martensite plates formed during storage and to rejuvenate the microstructure. The austenite grain boundaries of the HT and NHT samples were revealed by using the hot Lichtenegger-Bloch etching [24] and the mean austenite grain size determined was 6 and 8 μm for the NHT and HT samples, respectively.

The influence of applied magnetic fields on the isothermal martensitic transformation was studied by measuring in-situ the total magnetization in the sample at three different transformation temperatures (213, 233, 253 K) with applied magnetic fields up to 4 T for the HT samples. For the NHT samples the kinetics were measured up to 9 T but only at one temperature of 233 K. Small test samples of dimensions $0.5\times2\times3$ mm^3 were used. The SQUID magnetization measurements were performed using a MagLab system (Oxford Instruments) and a MPMS-XL system (Quantum design). To convert the magnetization measurements into the transformed martensite volume fraction it is necessary to have a reference value for a completely transformed sample. For this purpose, a cold rolled sample with a known volume fraction of martensite, (95% martensite, 5% Chi phase) was used. In this sample, all the austenite present in the initial microstructure was transformed into martensite by plastic deformation. From the saturation magnetization of the sample (M_{CR}), the saturation magnetization of 100%

martensite, M_{SAT}, can be easily derived (Table 2). The amount of martensite present in the initial microstructure of HT and NHT samples was extracted from the magnetization curve of each sample by dividing the saturation magnetization of the samples by M_{SAT}. Table 2 presents the initial volume fraction of martensite, f_i, in HT and NHT samples. The saturation values already show that the initial amount of martensite in the NHT sample is higher than for the HT. This could be expected, since the NHT samples have been at room temperature for several months before doing the experiments (at room temperature martensite also forms isothermally), while the HT was annealed to high temperatures at which the martensite retransforms to austenite.

Another important feature of the transformation behavior of this steel is the maximum amount of martensite that can be isothermally transformed ($f_S = 0.7$, as mention in the introduction of this work). In the present work it is assumed that this value is not dependent on the test temperature, the applied magnetic field or on the pre-heat treatments, so the same value will be adopted for all the samples under study.

For the metallographic examination of the martensite fraction in the isothermally transformed samples in the absence of an applied magnetic field, the samples were annealed at 823 K for 30 minutes, then mounted in bakelite and polished in the usual way, finishing in 1 μm diamond paste. Martensite was then revealed using hot Lichtenegger-Bloch etching solution [24]. The determination of the martensite volume fraction on these samples was done by the point counting method [25].

3. Kinetic model for the isothermal formation of martensite

The growth of martensite plates is so fast that this transformation is basically controlled by the nucleation rate [26]. Thus, growth is considered instantaneous and the volume of the martensite units is generally approximated as constant or as weakly varying with temperature or time. Several authors have observed that the IMT is characterized by a strong autocatalytic effect due to the generation of additional nucleation sites upon the formation of new martensitic plates [27]. The growth of martensite plates stops only at austenite grain boundaries or at existing martensite plates. An example of the martensitic plate arrangement in a partially transformed austenite grain for the steel studied is shown in Figure 1.

Considering the above mentioned transformation features, Shih et al [28] were the first to consider a rate equation to study the nucleation of martensite where all potential nucleation sites have the same activation energy: $dN/dt = n_i \nu \exp(-Q/RT)$; with N the number of martensitic plates formed per unit volume, t the time, n_i the total number density of preexisting embryos in the austenitic matrix at the start of the transformation, ν the attempt frequency, T the absolute temperature, R the ideal gas constant and Q the activation energy for the nucleation of a martensite plate. Raghavan and Entwistle [27] proposed a different expression to describe the total number of nucleation sites available anytime during the transformation and made it volume fraction dependent by introducing the autocatalytic factor p: $n = (n_i + pf - N)$, where f is the volume fraction of martensite. Pati and Cohen [29] included the "consumption" factor $(1-f)$ used as a prefactor in $n_i \nu \exp(-Q/RT)$. The impingement term $(1-f)$ reduces the number of potential nucleation sites and thereby the nucleation rate due to the austenitic regions

already transformed into martensite. Pati and Cohen [29] maintain in their formation a redundant term, "-*N*" (sites consumed by activation), which has not been taken into account in the present computations. Assuming that the plates of martensite have an average volume, V_M, that is assumed constant during the transformation, a general rate equation is obtained for the time evolution of the volume fraction of martensite,

$$\frac{df}{dt} = V_M \left(n_i + pf\right)\left(f_S - f\right)^X \nu \exp\left(\frac{-Q}{RT}\right), \tag{1}$$

This equation can be re-written in a more compacted way,

$$\frac{df}{dt} = \frac{1}{\tau}\left(1 + p_n f\right)\left(f_S - f\right)^X, \tag{2}$$

With

$$\tau = \frac{\exp\left(\frac{Q}{RT}\right)}{V_M \nu n_i}, \tag{3}$$

$$p_n = p/n_i, \tag{4}$$

Note that, with this formulation, p_n is the number of additional nuclei generated per martensitic nucleation event, which should never be below zero. In Eqs. (1)-(2), $X = 2$ [17, 30]. Eq (2) can be analytically solved, provided that V_M and Q are constant during the transformation (and assuming n_i and ν also constant), by separation of variables and by integrating f and t in the ranges $f_i \le f \le f_S$ and $t \ge 0$, respectively. Thus the following expression can be obtained,

$$\frac{t}{\tau} = \left(\frac{1}{1 + p_n f_S}\right)\left[\frac{1}{f_S - f} - \frac{1}{f_S - f_i}\right] + \frac{p_n}{\left(1 + p_n f_S\right)^2} \ln\left[\frac{\left(1 + p_n f\right)\left(f_S - f_i\right)}{\left(1 + p_n f_i\right)\left(f_S - f\right)}\right] \tag{5}$$

These equations will be used to interpret the kinetic results shown in Figures 2-4.

4 In-situ Magnetization measurements. Determination of the experimental activation energy for the nucleation of martensite, Q

Figures 2-4 show the time evolution of the volume fraction of martensite for NHT and HT samples for different experimental conditions. Figure 2 shows the influence of magnetic fields up to 9 T for NHT samples at 233 K; Figure 3 shows the influence of varying the isothermal testing temperature for constant applied fields of 2 T (a) and 4 T (b).

Figures 2 and 3 show that by increasing the applied magnetic field the kinetics of isothermal formation of martensite for both NHT and HT samples is accelerated significantly. It is very interesting to see that a shift in the test temperature of only 20 K (from 233 to 253 K) influences the kinetics very strongly. Figure 3 shows that the fastest kinetics occurs at 233 K followed by 213 K, and the slowest is found at 253 K; this is in agreement with a previous observation in the absence of applied magnetic fields [12]. Kakeshita and co-workers [16] observed that external applied magnetic fields were able to shift the nose of the curve at a rate of around 1 K/T in a Fe-Mn alloy. The applied magnetic fields used in this work are too weak to produce a detectable shift in the nose temperature for the present resolution in isothermal transformation temperatures of 20 K.

Equations (1)-(5) were used to fit the experimental results. Finding appropriate values for the different parameters in the equations represented an important challenge. In previous works found in the literature, n_i and V_M are usually taken as constants, for a constant grain size. Once these parameters are set, p_n and Q can be obtained. The value of n_i used by previous authors varies from 10^{10} to 10^{13} m^{-3} [26-28]. These values have been used even for austenite grain sizes as small as 10 μm, although for $n_i = 10^{13}$ m^{-3}

approximately only one out of every 100 grains in the microstructure would contain a potential nucleation site. Those authors suggest that the transformation expands thanks to the spreading-out of nucleation to neighboring untransformed grains by autocatalytic stimulation across the grain boundaries [31]. When using similar values as previous authors (V_M = 10^{-16}-10^{-17} m^3 and n_i = 10^{13} m^{-3}) it was found in the present work that the p_n value obtained was for most cases negative (physically not possible) or the product $p_n f$ much smaller than 1 in the range of volume fractions studied. Even if values up to n_i =10^{16}-10^{17} m^{-3} were used, similar results were obtained. Pati and Cohen [29] found in an Fe-Ni-Mn alloy that for a range of grain sizes (20-43 μm), at 190 K, the autocatalytic contribution was so weak that the nucleation rate was solely controlled by n_i; however, under these conditions they still used n_i = 10^{10} m^{-3} which for a grain size of 20 μm means that only 1 embryo is present every 10000 grains of austenite. Clearly, the accuracy of the published values for the pre-exponential factors is questionable. Given the numerical results obtained from equations (1)-(5), these are not applicable to the present case in that form because factor p_n looses all its meaning, which is the encouragement of new nucleation sites due to the formation of martensite (not to deplete them, $p_n < 0$). The results suggest that for the present steel and the experimental conditions employed in this work, the autocatalysis does not play an important role in the transformation. Therefore, equation (5) has been simplified by making the approximation $p_n = 0$, leading to

$$\frac{t}{\tau} = \left[\frac{1}{f_S - f} - \frac{1}{f_S - f_i} \right], \qquad (6)$$

From the slope of the curve obtained by plotting $1/(f_S - f)$ vs time, *t*, for known values of V_M, n_i and ν, the activation energy of the process can be deduced. The volume of the martensite plates has been estimated by assuming the plates to be oblate spheroids ($V_M = 4\pi c^2 a/3$). Most of the quantitative metallography related to the measurement of the semithickness to radius ratio (c/a) of martensite plates concerns Fe-Ni-Mn alloys [28, 29, 32]. Raghavan and Entwistle [27] found that $c/a = 20$ independently of the grain size, while Pati and Cohen [29] measured that it actually varies from 10 to 26 when the grain size is varied from 10 to 190 μm. Ghosh and Raghavan [32] found that c/a increases with decreasing isothermal formation temperature (from 13 at 193 K to 25 at 77 K). In this work a constant value of $c/a = 9$ will be used for both for NHT and HT samples, based on the expected value extracted from the experimental results of of Pati and Cohen, with $c = 0.67L$ [29, 33]; thus, $V_M = 0.140L^3$, with L the austenite grain diameter metallographically determined. The attempt frequency has a value of $\nu = 10^7$ s^{-1} [4]. Since the autocatalytic effect has been found to be very weak, and it will not be taken into account here, theoretically every austenite grain should contain, from the beginning of the transformation, some potential embryos. If we consider an average number of *z* embryos present per austenite grain in the initial microstructure, then: $n_i = z/V_{GS}$, where V_{GS} is the average austenite grain volume. If grains are considered as tetrakaidecahedrons in three dimensions, then it can be deduced that $V_{GS} = 1.054L^3$ [34, 35]. Thus, compiling the previous expressions, $V_M \cdot n_i = z \cdot V_M / V_{GS}$. As $V_{GS}/V_M \approx 8$ gives an estimation of the average number of plates of martensite transformed per average austenite grain; hence $z > 8$. In this work, a value of $z = 16$ has been used for all samples, which is double the

expected number that will finally transform to a fully grown plate of martensite. Since c/a is taken as constant and independent of the grain size, then the product $V_M \cdot n_i$ remains also independent of the grain size. A good correlation was found between Eq. (6) and the experimental values. The solid lines in Figures 2-4 represent the fitting obtained according to this equation. Table 3 shows the activation energies obtained for the different experimental conditions after the fitting procedure. The standard deviations are also given in this table for every value of *Q*.

5 Theoretical model for the calculation of the activation energy for the nucleation of isothermal martensite under the influence of magnetic fields

Ghosh and Olson (G-O) [4] have developed a model to calculate the activation energy for the isothermal formation of martensite based on the analogy between slip deformation and martensitic transformations. This model considers that for the nucleation of isothermal martensite the stress to move a dislocation has not only an athermal contribution (as for the AMT) but also a thermal component (given by the time dependence of nucleation). The effect of point defects on the movement of dislocations at the martensitic interfaces during the nucleation and growth of martensite plates was treated in similar way. Based on their own previous work [36] they proposed the following expression for ferrous alloys,

$$Q = Q_0\left[1-\left(\Delta G_n/\Delta\hat{G}\right)^{1/2}\right]^{3/2} \qquad (7)$$

Where Q_0 is the height of the obstacles (the activation energy in the absence of driving force). Some authors have reported temperature dependent values between 29 and 145 kJ/mol [36] although if the motion of dislocations was the only rate controlling process,

Q_0=165 kJ/mol [38, 39] would be expected. In this work the experimentally determined value by G-O for high alloyed steels will be used (116 kJ/mol [4]). In Eq. (7), ΔG_n is the net molar driving force,

$$\Delta G_n = \Delta G_{ch} + \Delta G_{mag}^{th} + W_\mu + K_1 \quad (8)$$

$$K_1 = G^{el} + 2V_{mol}\sigma / nd \quad (9)$$

and $\Delta\hat{G}$ is the thermal frictional energy that has the same value as ΔG_n when the activation energy goes to zero and spontaneous growth can occur. In Eqs (8)-(9), ΔG_{ch} is the molar chemical free energy difference between austenite and martensite, ΔG_{mag}^{th} is the theoretical Gibbs energy contribution due to the applied magnetic field, W_μ is the athermal frictional energy, G^{el} is the molar elastic strain energy, V_{mol} is the molar volume of austenite, σ is the semi-coherent interfacial energy, n is the number of close-packed planes along the nucleus thickness and d is the spacing between close packed planes. The theoretical expression of parameters $\Delta\hat{G}$ and W_μ in equation (8) can be found elsewhere [3, 4]. These two parameters depend only on the concentration of the steel.

Previous studies on the influence of magnetic fields on the athermal formation of martensite [16, 18, 20] have shown that the magnetic contribution to the total free energy can be calculated by $\Delta G_{mag}^{th} = -V_m \Delta M \mu_0 H$ [20, 40], with μ_0 the permeability in vacuum ($4\pi\times10^{-7}$ N/A^2), V_m the molar volume of austenite (6.8×10^{-6} m^3/mol) and ΔM is the difference in the saturation magnetization between austenite and martensite and H the applied magnetic field (in units of A/m). Since austenite has a magnetization saturation

value much lower than martensite, it is assumed that $\Delta M \approx M_{SAT}$. Therefore, for the steel studied,

$$\Delta G_{mag}^{th} = -8.44\mu_0 H \tag{10}$$

with $\mu_0 H$ the applied magnetic field (in Tesla). Substituting equations (8)-(10) into equation (7) yields,

$$\left[1-\left(\frac{Q}{Q_0}\right)^{2/3}\right]^2 = -\frac{8.44}{\Delta\hat{G}}\mu_0 H + \frac{\left(K_1 + W_\mu + \Delta G_{ch}\right)}{\Delta\hat{G}}. \tag{11}$$

This equation has been used to study the dependence of the experimental activation energies with temperature and applied magnetic field. According to Eq. (11) and assuming that the magnetic contribution to the Gibbs free energy can be described by Eq. (10), the slope of the plot $\left[1-\left(Q/Q_0\right)^{2/3}\right]^2$ vs $\mu_0 H$ should be equal to $-8.44/\Delta\hat{G}$. Note that since $\Delta\hat{G}$ has a negative value, the slope of this plot is positive.

Figure 4 shows the variation of $\left[1-\left(Q/Q_0\right)^{2/3}\right]^2$ with the applied magnetic field. The solid lines represent the linear approximation. Please note that the slope of the HT samples has been taken as equal to that of the NHT ones as differences in Chi-phase levels and hence austenite composition are negligible. From the slope, *m*, the value of $\Delta\hat{G}$ has been deduced according to $\Delta\hat{G} = -8.44/m$. Table 4 compares the value obtained in this work and that obtain by G-O model. Our result indicates that in this steel there is a much lower thermal frictional energy than that predicted by G-O. Conversely, G-O model would imply that $\mu_0 M_{SAT} = 2.69T$ which is not in agreement with experiments. However, given the highly approximate nature of the equation to calculate the frictional work, the differences between the experimental and predicted value is acceptable.

As for $\Delta\hat{G}$ and W_μ, the value of ΔG_{ch} is solely composition dependent and should be similar for the HT and NHT samples. Thus, in this model only the energy term K_1 is susceptible to the influence of high temperature heat treatments, due to changes in the microstructure. From the intercept term in Figure 4, the value of K_1 can be obtained (Table 5) if ΔG_{ch} and W_μ are known. From the work of G-O, W_μ=957 J/mol for this steel [4] and ΔG_{ch} (Table 5) is obtained by using ThermoCalc Software [41]. Since the value of $\left[1-\left(Q(\mu_0 H=0)/Q_0\right)^{2/3}\right]^2$ has not been experimentally determined for the HT samples, it has been extracted from the linear fitting (Figure 4) as the value at the origin ($\mu_0 H=0$). The K_1 values experimentally obtained almost double the value obtained by G-O work (1010 J/mol) and seem to vary depending on the isothermal test temperature. The difference might partially lay on the different thermodynamic databases used. G-O used their own thermodynamic database developed at the Notherwestern University (based on SGTE-SSOL database) while here the TCFE3 database of ThermoCalc is used. Finally, the results at 233 K show that the application of a high temperature heat treatment promotes the transformation by lowering the energy necessary to form a nucleus of martensite. Taking typical values from the literature for G^{el} (450 J/mol [4]); σ (~0.15 J/m^2 [3]) and d (plane (111) in the fcc austenitic lattice, d=2.15×10^{-10} m), the defect size or number of close-packed planes comprising a nucleus thickness, n, can be estimated. In this work a value of n=6-7 has been obtained, which compares well with earlier estimates for Fe-Mn based alloys (n=8) and for Fe-Ni-Cr-Mn alloys (n=16-18) [4, 42].

6. Conclusions

In this work the influence of applied magnetic fields on the isothermal formation of martensite has been studied in samples with two different initial microstructures (HT and NHT) by measuring in-situ the total magnetization in the sample. From this work the following conclusions can be extracted:

1) It has been shown that applied magnetic fields strongly accelerate this transformation.

2) The activation energies for the nucleation of isothermal martensite have been derived by curve-fitting the experimental results using a semi-empirical kinetic model. The Ghosh and Olson model describes the time and field dependences of the activation energies derived reasonably well, it has been found that the thermal frictional energy ($\Delta\hat{G}$ =-1847 J/mol) and the defect size (n=6-7) are lower than those derived by these authors (-3188 J/mol and 16-18 respectively). Given the approximate nature of the equation used to calculate the thermal frictional work by Ghosh and Olson and the different thermodynamic database used in the present work compare to the work these authors, the differences found between the experimental and predicted values are acceptable.

7. Acknowledgements

The authors are grateful to the *Stichting voor Fundamenteel Onderzoek der Materie* (*FOM*) and the Netherlands Institute for Metals Research (*NIMR*) in the Netherlands for providing financial support. The support of Xu Wei with the thermodynamic calculations is greatly appreciated. The authors would also like to thank Jan Post, Manso Groen and

Henk Visser, from Philips Drachten in The Netherlands, for providing experimental support.

8. References

[1] H. K. D. H. Bhadeshia and R. W. K. Honeycombe, Steels: Microstructure and Properties, Butterworth-Heinemann, Oxford (2006) 112.

[2] J. W. Christian, Theory of Transformations in Metals and Alloys, Pergamon (2002) 1062,

[3] G. Ghosh, G.B. Olson, Acta Metall. Mater. 42 (1994) 3361.

[4] G. Ghosh, G.B. Olson, Acta Metall. Mater. 42 (1994) 3371.

[5] A. Borgenstam, M. Hillert, Acta Mater. 45 (1997) 651.

[6] V. A. Lobodyuk, E. I. Estrin, Physics-Uspekhi 48 (2005) 713.

[7] V. Raghavan, Martensite, Edited by G.B. Olson and W.S. Owen, ASM Internacional, Materials Park, Ohio (1992) 197.

[8] C. J. Slunder, A. F. Hoenie, A. M. Hall. Thermal and Mechanical Treatment for precipitation-hardening stainless steel. Columbus, Ohio: Clearinghouse (1968).

[9] M. Hattestrand, J-O. Nilsson, S. Krystyna, P. Liu, M. Andersson, Acta Mater. 52 (2004) 1023.

[10] J. Post, PhD, On the constitutive Behavior of Sandvik Nanoflex, University of Twente, 2004.

[11] S. O. Kruijver, H.S. Blaauw, J. Beyer, J. Post, J.Phys. IV France, 112 (2003) 437.

[12] M. Holmquist, J.-O Nilsson, A. H. Stigenberg, Scripta Metall. Mater. 33 (1995) 1367.

[13] J. Post, K. Datta, J. Huetink, AIP Conference Proceedings, 712 (2004) 1670.

[14] J. Post, J. Huetink, H. J. M. Geijselaers, R. M. J. Voncken, J. Phys. IV France, 112 (2003) 417.

[15] T. Kakheshita, T. Saburi, K. Shimizu, Mater. Sci. Eng. A273 (1999) 21.

[16] T. Kakeshita, Y. Sato, T. Saburi, K. Shimizu, Y. Matsuoka, K. Kindo and S. Endo, Mater. Trans. JIM 40 (1999) 107.

[17] D. San Martin, N.H. van Dijk, E. Bruck and S. van der Zwaag, Mater. Sci. Eng. A (2007), doi:10.1016/j.msea.2006.11.177.

[18] T. Kakeshita, K. Shimizu, Mater. Trans. JIM 38 (1997) 668.

[19] Y. Kurita, S. Emura, K. Fujita, K. Nagai, K. Ishikawa, K. Shibata, Fusion Eng. Design 20 (1993) 445.

[20] K. Shimizu, T. Kakeshita, ISIJ International 29 (1989) 97.

[21] J. K. L. Lai, C.H. Shek, Y.Z. Shao, A.B. Pakhomov, Mater. Sci. Eng. A379 (2004) 308.

[22] D San Martin, N. H. van Dijk, E. Bruck, S. van der Zwaag, Mat. Sci. Forum 500-501 (2005) 339.

[23] J. S. Kasper, Acta Metall. 2 (1954) 456.

[24] D. San Martin, P. E. J. Rivera Diaz del Castillo, E. Peekstok, S. van der Zwaag, Mater. Char. 58 (2007) 455.

[25] Standard Test Method for Determining Volume Fraction by Systematic Manual Point Count, ASTM 562-02.

[26] E. S. Machlin, M. Cohen, Trans. AIME 194 (1952) 489.

[27] V. Raghavan, A.R. Entwisle, Special Report No. 93, Iron and Steel Institute (London), 1965, 30.

[28] C. H. Shih, B. L. Averbach, M. Cohen, Trans. AIME 203 (1955) 183.

[29] S. R. Pati, M. Cohen, Acta Metall., 17 (1969) 189.

[30] J. B. Austin, R. L. Rickett, Trans. AIME 135 (1939) 396.

[31] V. Raghavan, Acta Metall. 17 (1969) 1299.

[32] G. Ghosh, V. Raghavan, Mater. Sci. Eng. A79 (1986) 223.

[33] S. R. Pati, M. Cohen, Acta Metall. 14 (1966) 1001.

[34] F. C. Hull, W. J. Houk, Journal of Metals (1953) 565.

[35] T. Gladman, The Physical Metallurgy of Microalloyed steels. The Institute of Materials, University Press, Cambridge (1997) 155.

[36] M. Grujicic, G. B. Olson, W.S. Owen, Metall. Trans A 16 (1985) 1713.

[37] G. Ghosh, V. Raghavan, Mater. Sci. Eng. A80 (1986) 65.

[38] G.F. Bolling, R.H. Richman, Philos. Mag. 19 (1969) 247.

[39] S. Kajiwara, J. de Physique C4 (1982) 97.

[40] H. D. Joo, J. K. Choi, S. U. Kim, N. S. Shin, Y. M. Koo, Metall. and Mater. Trans. A35 (2004) 1663.

[41] TCFE3-Thermo-Calc Steels/Fe-alloys database (Version 3.0), Royal Institute of Technology, Foundation of Computational Thermo-dynamics, Stockholm/Sweden, 2002.

[42] G. Ghosh, The Critical Driving Force for heterogeneous martensitic nucleation in solid solution strengthened alloys, Solid-solid Phase Transformations, Edited by W.C. Johnson, J.M. Howe, D.E. Laughlin and W.A. Soffa, The Minerals, Metals & Materials Society (1994) 691.

Figures

Figure 1 Surface relief formed by transformed martensite plates during isothermal transformation at 233 K on a polished surface of the studied steel. The dashed line approximates the austenite grain boundary.

Fig. 2 Isothermal evolution of the volume fraction of martensite at 233 K under the influence of different applied magnetic fields in samples NHT. Solid lines represent the fitting according to Eq. (6).

Fig. 3 Isothermal formation of martensite at different applied magnetic fields; a) 4 T and b) 2 T for HT samples. Solid lines represent the fitting according to Eq. (6)

Fig. 4 Variation of the reduced activation energy ($\left[1-\left(Q/Q_0\right)^{2/3}\right]^2$), first term in Eq. (11)) with magnetic field. The solid lines represent the linear fitting.

Tables

Table 1. Chemical composition of the studied steel [wt.%] with Fe to balance.

Cr	Ni	Mo	Ti	Al	Si	Cu	Mn	C, N
12.0	9.0	4.0	1.0	0.7	0.3	2.0	0.3	<0.01

Table 2. Values of different experimental parameters used in this work.

$\mu_0 M_{CR}$, T	$\mu_0 M_{SAT}$, T	f_i (NHT)	f_i (HT)	f_S [22]
1.479	1.559	0.026	0.009	0.7

Table 3. Activation energies Q (kJ/mol) for martensite nucleation.

$\mu_0 H$, T / T, K → ↓	233-NTH	213-HT	233-HT	253-HT
0	58,2±0.2	-	-	-
2	56,0±0.1	51,1±0.1	55,7±0.1	62,8±0.1
4	55,0±0.1	48,9±0.1	53,5±0.1	61,1±0.1
6	54,0±0.1	-	-	-
9	50,7±0.1	-	-	-

Table 4. gives the value of $\Delta\hat{G}$ compared to the one obtained from Ghosh-Olson's Theory.

	Experimental	G-O
$\Delta\hat{G}$, J/mol	-1847	-3188

Table 5. Chemical Gibbs free energy obtained from ThermoCalc software [38] and K_1 value obtained by fitting the experimental results to Eq (11).

T, K	ΔG_{ch} (ThermoCalc, J/mol)	K_1 (NHT samples, J/mol)	K_1 (HT samples, J/mol)
213	-3277	---	1995
233	-3148	1932	1920
253	-3017	---	1863

Figures

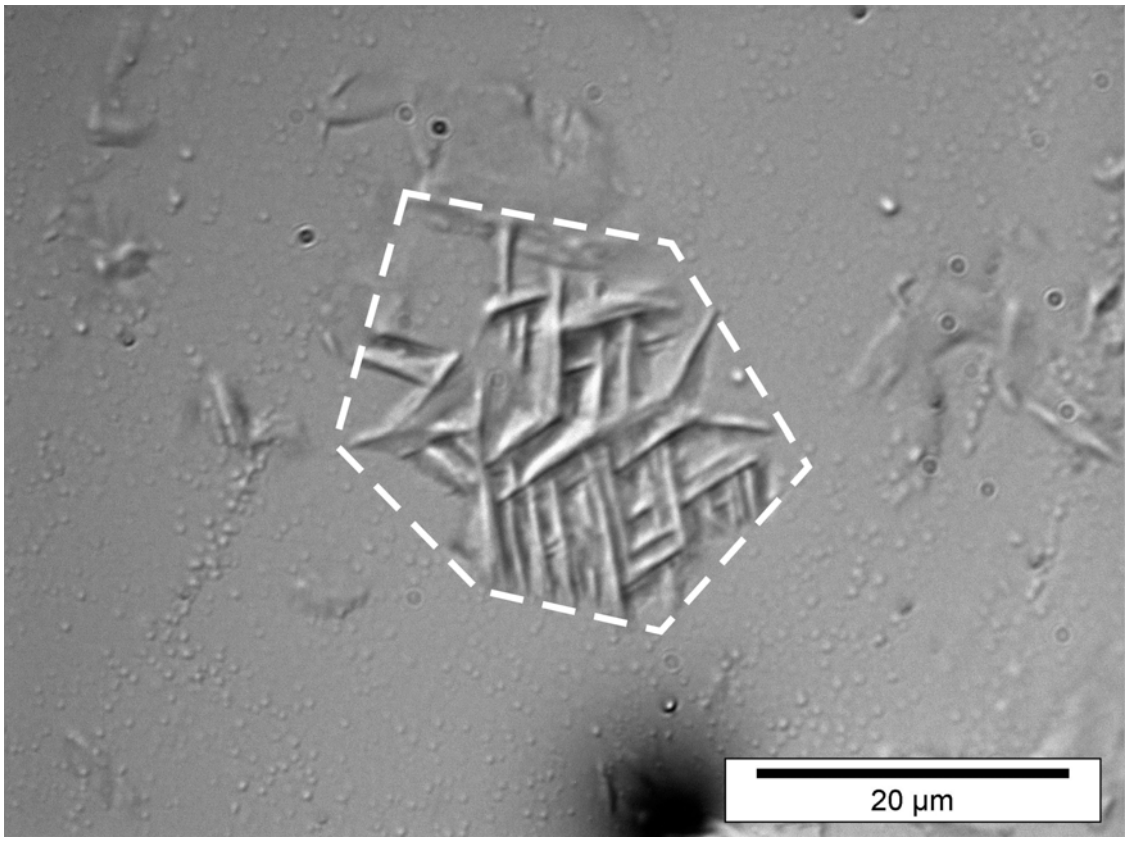

Figure 1 Surface relief formed by transformed martensite plates during isothermal transformation at 233 K on a polished surface of the studied steel. The dashed line approximates the austenite grain boundary.

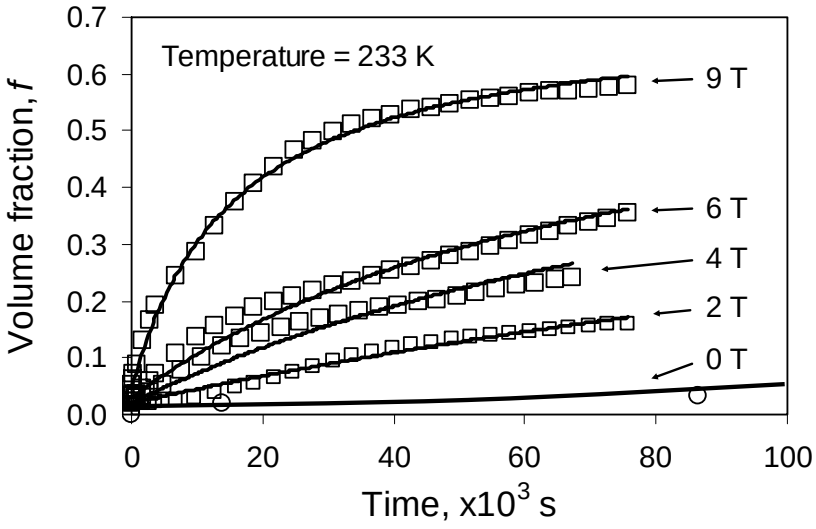

Figure 2 Isothermal evolution of the volume fraction of martensite at 233 K under the influence of different applied magnetic fields in samples NHT. Solid lines represent the fitting according to Eqs (6)-(7)

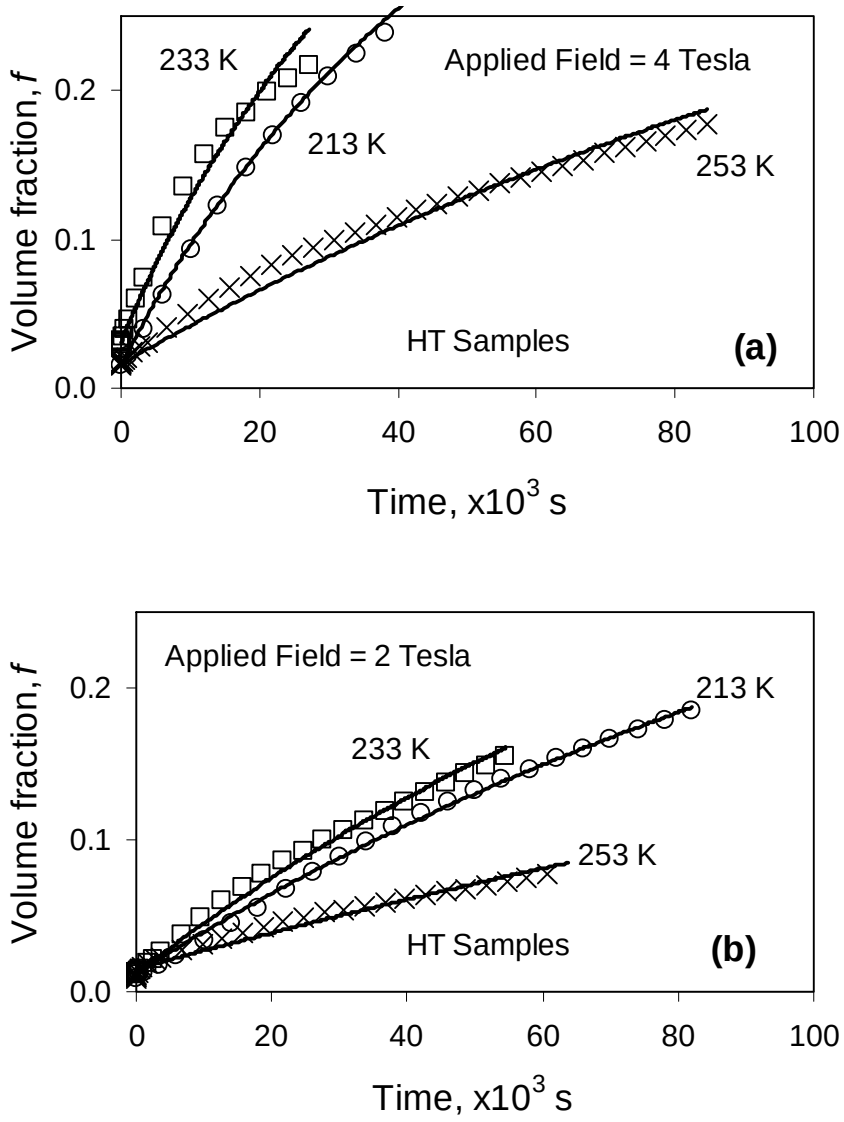

Figure 3 Isothermal formation of martensite at different applied magnetic fields; a) 4 T and b) 2 T for HT samples. Solid lines represent the fitting according to Eqs. (5)-(6)

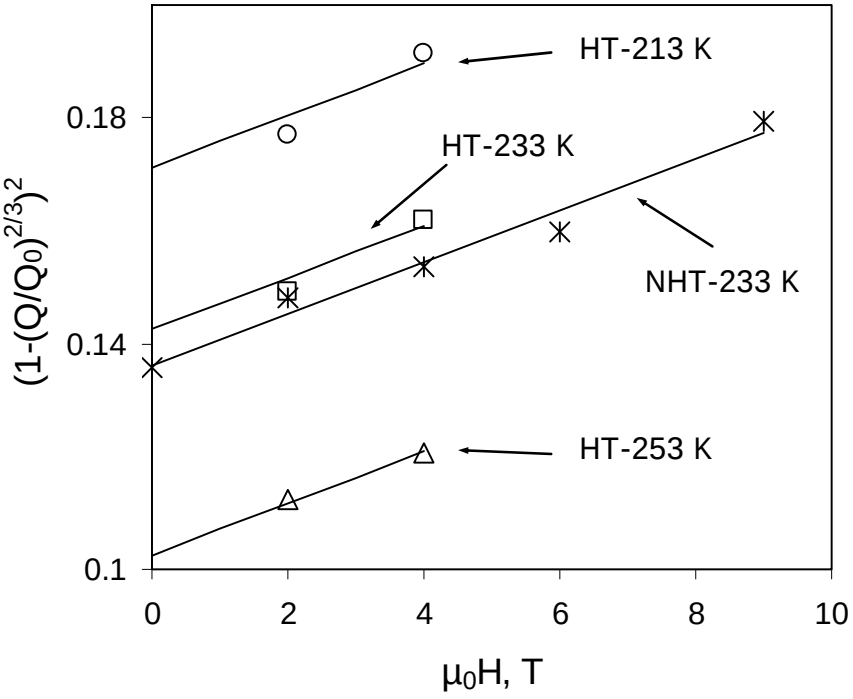

Figure 4 Variation of the reduced activation energy ($\left[1-\left(Q/Q_0\right)^{2/3}\right]^2$), first term in Eq. (12)) with magnetic field. The solid lines represent the linear fitting.